

Multimodal Semi-Supervised Learning for Text Recognition

Aviad Aberdam¹, Roy Ganz^{2*}, Shai Mazor¹, and Ron Litman¹

¹ AWS AI Labs

² Technion, Israel

{aaberdam,smazor,litmanr}@amazon.com, ganz@cs.technion.ac.il

Abstract. Until recently, the number of public real-world text images was insufficient for training scene text recognizers. Therefore, most modern training methods rely on synthetic data and operate in a fully supervised manner. Nevertheless, the amount of public real-world text images has increased significantly lately, including a great deal of unlabeled data. Leveraging these resources requires semi-supervised approaches; however, the few existing methods do not account for vision-language multimodality structure and therefore suboptimal for state-of-the-art multimodal architectures. To bridge this gap, we present semi-supervised learning for multimodal text recognizers (SemiMTR) that leverages unlabeled data at each modality training phase. Notably, our method refrains from extra training stages and maintains the current three-stage multimodal training procedure. Our algorithm starts by pretraining the vision model through a single-stage training that unifies self-supervised learning with supervised training. More specifically, we extend an existing visual representation learning algorithm and propose the first contrastive-based method for scene text recognition. After pretraining the language model on a text corpus, we fine-tune the entire network via a sequential, character-level, consistency regularization between weakly and strongly augmented views of text images. In a novel setup, consistency is enforced on each modality separately. Extensive experiments validate that our method outperforms the current training schemes and achieves state-of-the-art results on multiple scene text recognition benchmarks. Code will be published upon publication.

Keywords: Scene Text Recognition, Semi-Supervised, Contrastive Learning, Consistency Regularization, Teacher Student

1 Introduction

Understanding written information through vision is essential to most of our everyday tasks, and as such, it is a key research area in artificial intelligence. For that reason, scene text recognition, which deals with text in natural environments, has been studied extensively in the past two decades [29,10,43]. Unfortunately, until recently, public real-world data for scene text have been fairly scarce,

* Work done during an Amazon internship.

leading the community to focus almost entirely on synthetic training data and hence on supervised training methods [44,45,26,62,27,4,58,55,53,59,28,38,60,34]. However, in recent years, the number of public real-world text images has increased significantly, including a few million unlabeled images. Therefore, as advocated by [5], it is time to focus on unsupervised and semi-supervised algorithms that can advantage these resources. Such methods, though, have been barely studied for text recognition [64,1,5,13], while the few that do exist do not account for the multimodal structure and therefore cannot fully leverage unlabeled data in advanced multimodal recognizers [56,13,38,59].

In this work, we present semi-supervised learning for multimodal text recognizers (SemiMTR). To this end, we adopt the ABINet [13] vision-language multimodal architecture and introduce a semi-supervised training scheme that utilizes unlabeled data at each modality training and therefore leverages the multimodal structure. Originally, ABINet is trained via three stages: (i) a supervised vision model pretraining; (ii) a bidirectional language representation learning of the language model; and (iii) a supervised fine-tuning of the fusion model and entire network. Our method offers different first and third steps for this procedure that can benefit from unlabeled real-world images. In contrast to leading semi-supervised text recognition approaches, which are based on pseudo-labeling and require additional retraining steps [5,13], our training procedure maintains the original three-stage scheme.

For pretraining the vision model, we harness both labeled and unlabeled data via contrastive learning, which, as we show, leads not only to improved performance of the vision model but also of the entire end-goal network. The key idea of contrastive-based methods is to maximize agreement between representations of differently augmented views of the same image and distinguish them from representations of other images [9,16]. This way, the visual backbone learns to concentrate on the image text content and ignore unimportant attributes, such as color, texture, and perspective. More specifically, we adapt SeqCLR [1], an existing sequence-to-sequence contrastive learning method, originally designed for handwriting recognition, and extend it to scene text recognition. For this goal, we adopt a more robust transformer-based backbone, apply stronger color-texture augmentations, which are essential to text-in-the-wild images, and present a single training stage that already contains the supervised training, which usually operates separately after. Our vision-model pretraining is the first contrastive method successfully applied to scene text images.

Our fine-tuning stage, which targets the final model predictions, presents a sequential, character-level, consistency regularization between weakly and strongly augmented views of real-world text images. Our scheme first generates a sequence of artificial pseudo-labels from a weakly-augmented text image and then uses it to train all modalities fed by a strongly-augmented view of the same image. Our study reveals that this learning is most beneficial when each modality is the teacher of itself and generates its pseudo-labels to train on.

We first validate our method experimentally against state-of-the-art synthetic-based methods and reveal that applying our algorithm only on real-world images

reduces the word error rate by 14% on widely-used scene text benchmarks and 28% on non-common ones. Our results are the first to surpass synthetic-based solutions and, thus, significantly strengthen the claim of [5] that real datasets have been accumulated to a sufficient level. In addition, we compare our scheme with existing semi-supervised methods and demonstrate improvements in the overall performance, enhancing the state-of-the-art on 12 out of 13 scene text recognition benchmarks. Finally, we provide a comprehensive analysis of our framework, exploring the impact of its components.

To summarize, the main contributions of our work are:

- A multimodal semi-supervised learning algorithm for text recognition, which is customized for modern vision-language multimodal architectures.
- A unified one-stage pretraining method for the vision model, which is the first successful contrastive learning scheme for scene text recognition.
- A sequential, character-level, consistency regularization in which each modality teaches itself.
- Extensive experiments demonstrate state-of-the-art performance on multiple scene text recognition benchmarks.

2 Related Work

Vision-language multimodal text recognizers. In the past few years, modern text recognition schemes have focused on extracting visual and semantic information encompassed in text images and balancing them together [38,59,28,13,56]. More specifically, SCATTER [28] proposed custom decoders for these two information types; SRN [59] introduced a global semantic reasoning module; SEED [38] offered a semantics enhanced encoder-decoder framework; and VisionLAN [56] endowed the vision model with language capability. Recently, ABINet [13] presented a vision-language multimodal architecture that possesses an explicit language model, which can be pretrained on some text corpus. Through a three-stage training procedure described in Section 3, ABINet reached state-of-the-art results on scene text recognition. Our work is the first to present a semi-supervised learning scheme that utilizes the vision-language structure in these modern text recognition methods.

Semi-supervised learning for text recognition. Untill recently, real-world public images of scene text were so rare, that the few to exist were used for evaluation. Therefore, most training methods [44,45,26,62,27,4,58,55,53,59,28,38,60,36] have been based on two large synthetic datasets [18,15] and have operated in a fully-supervised fashion. Exceptions to this are [64] and [21], which suggested sequence-to-sequence domain adaptation techniques between labeled and unlabeled datasets, and [1] which introduced a sequence-to-sequence contrastive learning for visual representations learning. In addition, [5,19,13] offered pseudo-labeling methods to utilize real-world unlabeled images, while the latter added a confidence-based criterion for filtering noisy pseudo-labels. Our work is the first

to propose semi-supervised learning for text recognition that utilizes the multimodal structure. To this end, we develop self-supervised learning methods for the vision model pretraining and the fine-tuning phase, based on representation learning and consistency regularization, respectively.

Consistency regularization. Consistency regularization is a widely-used technique in self-supervised learning. Its core idea is that the model predictions should remain the same under each semantic-preserving perturbations of the same image. Many works [3,42,24,50,6,57] introduce mechanisms to impose consensus on the network outputs. For example, [42] enforces the network to be agnostic to some transformations and disturbances, and [57] proposes a consistency regularization in semi-supervised settings by using noise injections and augmentations on the unlabeled examples. A more closely-related work to our proposed method is FixMatch [48]. This paper integrates consistency regularization with pseudo-labeling to benefit from unlabeled data in classification tasks. More specifically, FixMatch trains the predictions from the strongly-augmented version to match the pseudo-label produced from the weakly-augmented view of the same image. Motivated by these papers, we propose a sequential, character-level, consistency regularization for the fine-tuning stage of the whole network, in which we enforce consistency on each modality separately. Our scheme, tailored for the modern multimodal architectures, outperforms current semi-supervised methods for scene text recognition.

3 Architectural Background

Throughout this work, we focus on the novel multimodal ABINet [13] architecture, on which we demonstrate our multimodal semi-supervised (SemiMTR) algorithm. As depicted in Fig. 1 and further detailed in Appendix A, ABINet architecture fuses the features of the vision model and the language model to obtain its final predictions. ABINet’s training scheme comprises three stages. The first stage is a fully-supervised pretraining of the vision model. Independently, we pretrain the language model on a large text corpus via a version of masked language modeling [12], in which we mask the attention maps instead of input characters. Finally, an end-to-end fine-tuning stage is applied via supervised cross-entropy losses on the vision, language, and fusion predictions. The following section describes our training method, which enables leveraging unlabeled text images in multimodal architectures.

4 SemiMTR: Multimodal Semi-Supervised Learning

We introduce SemiMTR, semi-supervised learning for multimodal text recognizers, which aims to fully utilize vision-language multimodal architectures by leveraging unlabeled data at each modality training. Our method offers an overall simple algorithm that maintains a three-stage training procedure as in ABINet supervised learning (see Section 3 above). Our vision model pretraining is

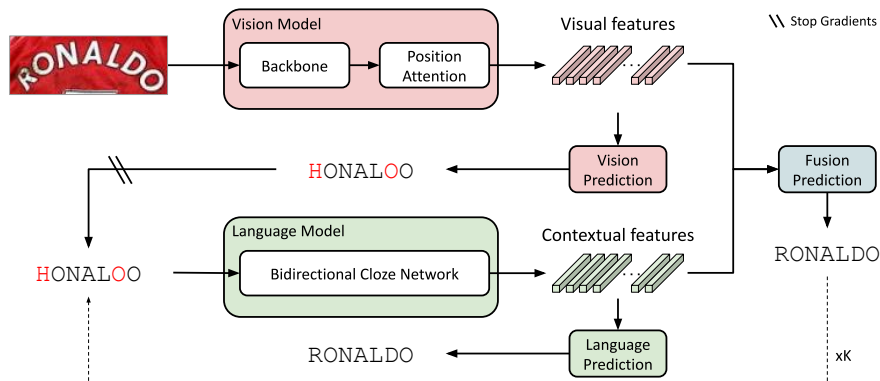


Fig. 1: **Text recognition architecture.** We adopt ABINet [13] as our case study of vision-language multimodal recognizers. In this scheme, the vision model first extracts a sequence of visual features from a given image and then decodes it into character predictions. Next, these predictions are fed to the language model, which derives contextual features. Finally, the fusion model operates on the visual and contextual features and provides the network final prediction. To further improve accuracy, an optional iterative phase, drawn with a dashed line, reinserts the output back to the language model as a predictions-refinement step

an extended version of the sequence-to-sequence contrastive learning [1], which we integrated with a supervised loss. Independently, the language modality is trained on a large text corpus using the same masked language modeling of ABINet [13]. For completeness, we further describe this step in Appendix B. Finally, the entire network is fine-tuned via a sequential, character-level, consistency regularization between weakly and strongly augmented views of the input images. We empirically find out that this regularization is the most effective when each modality is the teacher of itself and creates its own pseudo-labels.

4.1 Vision Model Pretraining

To better utilize unlabeled real data, we propose including these resources also during the vision model pretraining. As our experiments show, such training not only improves the accuracy of the vision model but eventually leads to better generalization of the final network and performance gain over competitive semi-supervised methods [13,5], which use unlabeled data only in the last training phase. These results indicate that the semi-supervised learning of the vision model is essential to fully benefit from unlabeled data in multimodal schemes.

As illustrated in Fig. 2, this stage harnesses unlabeled data by performing unsupervised visual representation learning along with supervised training. In particular, we extend the sequence-to-sequence contrastive learning framework (SeqCLR) [1] to scene text recognition and transformer-based backbone and unify it with supervised training. Interestingly, as experimented in Section 6.1,

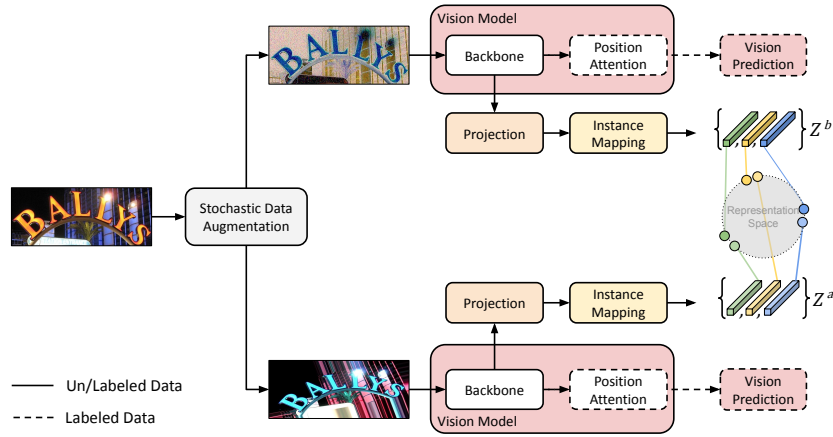


Fig. 2: **Visual representation learning for vision model pretraining.** Our method augments twice each image in a batch and feeds these views into a visual backbone and projection head. Next, we apply an instance-mapping function [1], which creates a sequence of representations for each augmented view and thus enables contrastive learning at a sub-word level. A parallel branch computes supervised loss on the visual predictions of the labeled data

integrating the visual representation learning with the supervised training into a single stage leads to performance gains. More specifically, our pretraining procedure consists of the following six building blocks:

- **Stochastic data augmentation**, which creates two augmented views for each input text image. The original augmentation pipeline proposed in SeqCLR [1] was mainly designed for handwritten-text images, in which the background is usually solid and of light colors. However, in scene text images, the background significantly varies between different images. Therefore, to obtain representations that focus on the foreground text and not the background, we propose stronger augmentations, especially in terms of the image color and texture. Note that the proposed augmentations preserve the sequential structure of the input to maintain alignment between the two sequences of representations that will be extracted from these augmented views. Fig. 3 in the “Strong” column presents augmentation pipeline demonstrations, and Appendix E provides its pseudo-code.
- **Visual backbone** extracts visual features out of the augmented images. Unlike SeqCLR [1], which applied representation learning merely to a convolutional neural network (CNN), here, we follow the leading text recognition methods [13,25,2] and adopt the visual backbone of ABINet [13], which consists of ResNet and Transformer units.
- **Projection head**, an optional auxiliary network, which transforms the visual backbone features into a lower-dimensional space.
- **Instance-mapping function**. A unique block for sequence-to-sequence predictions divides each feature map into a sequence of separate representations

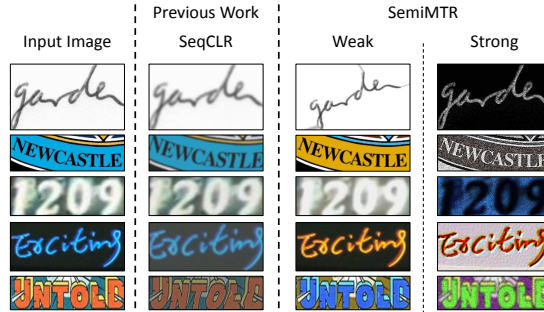


Fig. 3: **Proposed augmentations.** The augmentation pipeline proposed by SeqCLR [1] is mainly designed for handwriting text images, in which the background is often solid and of light colors. See an example in the first row. However, the background of scene text images varies significantly between different instances, as illustrated in the last four rows. Therefore, to enforce the learned representation to concentrate on the text content and not the image visual attributes, we propose higher severity augmentations, especially in terms of image color and texture

over which the contrastive loss is computed. This operation enables contrasting between individual elements of the sequence and not whole images, as in standard contrastive methods [9,16,14,8]. We adopt the window-to-instance mapping approach [1], in which a batch of (possibly projected) feature maps, $\mathbf{P} \in \mathbb{R}^{N \times F \times H \times W}$, is first flattened to the shape of $\mathbb{R}^{N \times H \cdot W \times F}$. Then, using the adaptive average pooling, we extract T separate representations out of each flattened feature map and collect them into a set \mathcal{Z} :

$$\mathcal{Z} = \text{AdaptiveAvgPool2d}(\text{Flatten}(\mathbf{P})). \quad (1)$$

This function is called twice for each augmented view of the input, resulting in two sets of representations, $\mathcal{Z}^a, \mathcal{Z}^b$.

- **Contrastive loss** aims to bring closer corresponding representations, termed positive pairs, and distinguish them from the others, denoted as negative examples. The contrastive loss is calculated over the two sets of representations extracted by the instance-mapping function, $\mathcal{Z}^a, \mathcal{Z}^b$, each of the size of NT :

$$\mathcal{L}_{\text{SeqCLR}}(\mathcal{Z}^a, \mathcal{Z}^b) = \sum_{0 \leq i < NT} \ell_{\text{NCE}}(\mathbf{z}_i^a, \mathbf{z}_i^b; \mathcal{Z}^a \cup \mathcal{Z}^b) + \ell_{\text{NCE}}(\mathbf{z}_i^b, \mathbf{z}_i^a; \mathcal{Z}^a \cup \mathcal{Z}^b), \quad (2)$$

where ℓ_{NCE} is the noise contrastive estimation (NCE) loss function [37]:

$$\ell_{\text{NCE}}(\mathbf{u}^a, \mathbf{u}^b; \mathcal{U}) = -\log \frac{\exp(\text{sim}(\mathbf{u}^a, \mathbf{u}^b)/\tau)}{\sum_{\mathbf{u} \in \mathcal{U} \setminus \mathbf{u}^a} \exp(\text{sim}(\mathbf{u}^a, \mathbf{u})/\tau)}, \quad (3)$$

with a temperature parameter τ and similarity operator of the cosine distance, $\text{sim}(\mathbf{v}, \mathbf{u}) = \mathbf{v}^T \mathbf{u} / \|\mathbf{v}\| \|\mathbf{u}\|$.

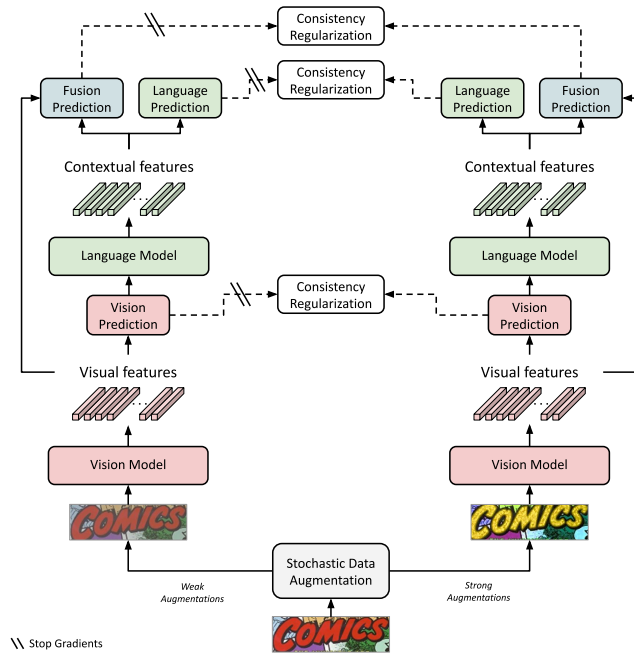


Fig. 4: **Sequential consistency regularization for model fine-tuning.** Our scheme generates a sequence of artificial pseudo-labels for each modality out of a weakly-augmented image (left). Then, a sequential, character-level, consistency regularization is computed for each modality separately between the above pseudo-labels and the modality predictions for a strongly-augmented view of the same image (right). We further calculate a supervised loss on the labeled data.

- **Vision decoder and supervised loss.** In SeqCLR [1] and standard contrastive learning methods [9,16,14,8], the supervised training phase occurs after the self-supervised stage ends. However, we refrain from increasing the overall training stages and offer an integrated, semi-supervised training scheme. Therefore, the overall loss of the vision model pretraining is:

$$\mathcal{L} = \lambda_U \sum_{\mathcal{D}_U, \mathcal{D}_L} \mathcal{L}_{\text{SeqCLR}} + \lambda_L \sum_{\mathcal{D}_L} \mathcal{L}_{\text{ce}}, \quad (4)$$

where $\mathcal{D}_U, \mathcal{D}_L$ are the unlabeled and labeled datasets, \mathcal{L}_{ce} is the cross-entropy loss on the visual decoder predictions, and $\lambda_U, \lambda_L \geq 0$ are scalar coefficients.

4.2 Consistency Regularization for Fusion Model Training

After pretraining the vision and language models, we move on to train the fusion model and fine-tune the entire network. Here, as well, we introduce a unified stage that combines both supervised and self-supervised training objectives. Therefore, this training offers a more efficient procedure than leading semi-supervised

methods [13,5], which are based on pseudo labeling and thus require retraining steps. For the self-supervised learning at this stage, we propose a sequential, character-level, consistency regularization, which better suits the nature of the fine-tuning phase. As demonstrated in Fig. 4, our method first generates a sequence of artificial labels out of a weakly-augmented version of the image and then uses them to train *all modalities* fed by a strongly-augmented view of the same input. Our work provides a comprehensive study of this stage, exploring each of the following components:

- **Stochastic strong and weak augmentations.** We fix the weak augmentation pipeline to be as used in ABINet [13] for supervised training. For the strong augmentations, we examine different techniques and find out that the color-texture augmentation method, proposed for our vision model pretraining, is the most efficient. See samples of these augmentations in Fig. 3.
- **Sequential consistency regularization loss** is computed between sequential predictions of weakly and strongly augmented views of the same input image. Our method first prunes the teacher’s sequential prediction at the first padding token location, denoted by N^{weak} . Then, it applies the consistency regularization on each character independently, using the configurable loss function of:

$$\mathcal{L}_{\text{Consist}}(\mathbf{Y}^{\text{strong}}; \mathbf{Y}^{\text{weak}}) = \sum_{0 \leq i < N^{\text{weak}}} \mathbf{1}(\max(\mathbf{y}_i^{\text{weak}}) > t) \ell(\mathbf{y}_i^{\text{strong}}, \mathbf{y}_i^{\text{weak}}), \quad (5)$$

where $\mathbf{Y}^{\text{strong}}, \mathbf{Y}^{\text{weak}}$ denote the sequential probability vectors of strongly and weakly augmented views, $\mathbf{1}(\cdot > t)$ is the threshold operator on $t \geq 0$, and ℓ is the core loss function, which in our case is cross-entropy or KL-divergence. In Section 6.2, we examine the effect of these ingredients, including the core loss function, the threshold, and the type of the teacher labels, \mathbf{Y}^{weak} – raw probability vectors versus one-hot labels.

- **Teacher and student modalities.** Usually, the teacher and student decoders on which the consistency regularization is computed are simply the same single decoder of the entire network. However, in multimodal text recognition schemes, each modality has its own decoder, and thus, can serve as either a teacher or a student. In Section 6.2, we further examine these different configurations and find out that each modality should generate its own pseudo-labels, namely, be its own teacher. Therefore, the loss can be formulated as follows:

$$\sum_{d \in \text{decoders}} \lambda_{U_d} \sum_{\mathcal{D}_U, \mathcal{D}_L} \mathcal{L}_{\text{Consist}}(\mathbf{Y}_d^{\text{strong}}; \mathbf{Y}_d^{\text{weak}}) + \lambda_{L_d} \sum_{\mathcal{D}_L} \mathcal{L}_{\text{ce}}(\mathbf{Y}_d^{\text{strong}}) + \mathcal{L}_{\text{ce}}(\mathbf{Y}_d^{\text{weak}}), \quad (6)$$

where $\text{decoders} = \{\text{vision, language, fusion}\}$, $\mathcal{D}_U, \mathcal{D}_L$ are unlabeled and labeled datasets, $\mathbf{Y}_d^{\text{strong}}, \mathbf{Y}_d^{\text{weak}}$ denote the probability maps of decoder d from strongly and weakly augmented views, $\mathcal{L}_{\text{ce}}(\cdot)$ is the supervised cross-entropy loss with the ground-truth labels, and $\lambda_{U_d}, \lambda_{L_d} \geq 0$ are coefficient scalars.

5 Experiments

In this section, we demonstrate the effectiveness of our method through extensive experiments, while our goal is two-fold. First, we aim to analyze the capability of current synthetic and real-world datasets. We show that applying our algorithm on real-world data surpasses all supervised synthetic-based methods, although real-world labeled data are only 1.7% of synthetic data. Our work is the first to achieve such results, whereas [5] only reached near but below state-of-the-art results. Specifically, our method reduces the word error rate by 14% on standard benchmarks and 28% on less common ones compared to ABINet [13]. That said, synthetic data is still valuable, and when harnessed with real-world data, it further reduces the word error rate by 12%. In addition, we compare our method with leading semi-supervised methods, which, for a fair comparison, are reimplemented and applied on the same training set. SemiMTR consistently outperforms these methods on multiple scene text benchmarks.

Datasets. We examine our method on multiple public datasets of scene text recognition, which we list in Table 1 and detail in Appendix D. We denote by *Real-L* and *Real-U* the real-world labeled and unlabeled training datasets, as defined by [5], and by *Synth* the synthetic datasets. Unlike several works which used the test set for validation, our validation set is a portion of the training partitions of Real-L dataset, as divided by [5]. In addition to the common six scene text benchmarks, IIIT [33], SVT [54], IC03 [30] IC13 [23], IC15 [22], SVTP [39] and CUTE [40], which we term *Common Benchmarks*, we also consider the test partitions of Real-L, which we term *Non-Common Benchmarks*. Our report provides word-level accuracy on each of these datasets and weighted averages on the common and non-common benchmarks. As a general statement, we believe that *as a community, we should expand the scope of the evaluation benchmarks*. The reason is that common benchmarks are pretty small, only 7.6K images overall, and therefore are insufficient and may lead to false scientific discoveries. The extreme case

is the CUTE dataset, 288 images, on which the accuracy is already higher than 90%, and therefore, new algorithms are measured on the misclassified examples, less than 30 images. On the other hand, adopting the non-common benchmarks significantly enlarges the test set and enriches its domain diversity.

Table 1: **Training datasets**

	Dataset	#Words
Real-L	SVT [54]	231
	IIIT [33]	1794
	IC13 [23]	763
	IC15 [22]	3,710
	COCO-Text [52]	39K
	RCTW [46]	8,186
	Uber-Text [65]	92K
	ArT [11]	29K
	LSVT [49]	34K
	MLT19 [35]	46K
	ReCTS [63]	23K
	Total	276K
Real-U	Book32 [17]	3.7M
	TextVQA [47]	463K
	ST-VQA [7]	69K
	Total	4.2M
Synth	ST [15]	7M
	MJ [18]	9M
	Total	16M

Table 2: **Scene text SOTA comparison.** Scene text recognition accuracies (%) over common and non-common public benchmarks. We show the number of words in each dataset below its title and present weighted (by size) average results on each set of datasets. The best performing result at each column is marked in bold. “*” refers to reproduced results and “Git” to GitHub model

Method	Labeled Data	Unlabeled Data	Common Benchmarks								Non-Common Benchmarks							
			IIIT 3,000	SVT 647	IC13 1,015	IC15 2,077	SVTP 645	CUTE 288	Avg. 7,672	COCO 9,835	RCTW 1,050	Uber 80,826	ArT 35,284	LSVT 4,257	MLT19 5,693	ReCTS 2,592	Avg. 139,537	
PlugNet [28]	Synth	✗	94.4	92.3	95.0	82.2	84.3	85.0	89.8	-	-	-	-	-	-	-	-	
RobustScanner [61]	Synth	✗	95.3	88.1	94.8	77.1	79.5	90.3	88.2	-	-	-	-	-	-	-	-	
SCATTER [28]	Synth	✗	93.7	92.7	93.9	82.2	86.9	87.5	89.7	-	-	-	-	-	-	-	-	
Plugnet [34]	Synth	✗	94.4	92.3	95.0	82.2	84.3	85.0	89.8	-	-	-	-	-	-	-	-	
SRN [59]	Synth	✗	94.8	91.5	95.5	82.7	85.1	87.8	90.3	-	-	-	-	-	-	-	-	
VisionLAN [56]	Synth	✗	95.8	91.7	95.7	83.7	86.0	88.5	91.1	-	-	-	-	-	-	-	-	
TRBA [4]	Synth	✗	92.1	88.9	93.1	74.7	79.5	78.2	85.7	50.2	59.1	36.7	57.6	58.0	80.3	80.6	46.3	
TRBA [5]	Real-L	✗	93.5	87.5	92.6	76.0	78.7	86.1	86.6	62.7	67.7	52.7	63.2	68.7	85.8	83.4	58.6	
TRBA _{PL} [5]	Real-L	Real-U	94.8	91.3	94.0	80.6	82.7	88.1	89.3	66.9	71.5	54.2	66.7	73.5	87.8	85.6	60.9	
TRBA _{PL} [5]	Real-L, Synth	Real-U	95.2	92.0	94.7	81.2	84.6	88.7	90.0	-	-	-	-	-	-	-	-	
TRBA _{PL} [5]	Real-L, Synth	Real-U	95.2	92.0	94.7	81.2	84.6	88.7	90.0	-	-	-	-	-	-	-	-	
ABINet ^{Git} [13]	Synth	✗	96.4	93.2	95.1	82.1	89.0	89.2	91.2	63.1	59.7	39.6	68.3	59.5	85.0	86.7	52.0	
ABINet* [13]	Real-L	✗	95.5	93.4	94.4	83.0	87.1	89.6	90.8	69.2	71.6	55.7	67.7	73.7	88.2	90.6	62.4	
ABINet _{PL} * [13,5]	Real-L	Real-U	96.4	94.1	95.0	83.7	88.8	93.1	91.8	71.2	74.2	56.8	70.5	75.0	89.1	90.9	63.9	
ABINet _{at} * [13]	Real-L	Real-U	96.5	96.3	95.7	83.7	89.1	92.0	92.1	71.7	73.8	56.8	70.1	75.7	89.3	91.6	63.9	
SemiMTR-V	Real-L	Real-U	95.6	93.5	95.2	82.5	88.1	90.6	91.0	70.5	75.1	57.7	69.5	75.2	89.6	92.3	64.2	
SemiMTR-F	Real-L	Real-U	96.5	95.4	96.5	84.2	89.6	90.6	92.3	70.9	74.9	57.7	70.3	75.5	89.3	91.5	64.4	
SemiMTR	Real-L	Real-U	96.7	95.5	96.6	83.8	90.5	93.8	92.4	72.0	75.8	58.5	70.8	77.1	90.3	92.5	65.2	
SemiMTR	Real-L, Synth	Real-U	97.3	96.6	97.0	84.7	93.0	93.8	93.3	72.7	76.3	58.4	72.3	77.1	90.2	93.2	65.6	

Implementation details. In many configuration parameters, such as architecture, optimizer, and image size, we follow the setting of ABINet [13]. A full description is provided in Appendix F.

Training time. A comparison with ABINet supervised training [13] shows that our vision model pretraining is longer by 65% (495K vs. 300K iterations), but our fusion model training is shorter by 65% (130K vs. 376K). Note that the latter training involves the whole network, and thus each iteration takes longer.

5.1 Comparison to State-of-the-Art Methods

Our study aims to probe the efficiency of current synthetic and real-world public datasets. Therefore, we start by comparing training on synthetic images to real-world labeled data. While synthetic data are relatively easy to acquire and lead to on-par performance on common benchmarks, they result in poor performance on the non-common benchmarks. See TRBA and ABINet results on Synth versus Real-L in Table 2. More specifically, ABINet trained on synthetic datasets achieves 52.0% on non-common benchmarks, compared to 62.4% of ABINet trained on Real-L. This observation, also reported by [5], demonstrates the potential of synthetic data, but simultaneously indicates that current public, synthetic data do not represent well the diversity of the non-common benchmarks.

Building upon this understanding, we move on to experiment methods that can leverage the unlabeled real-world datasets (Real-U). To this end, we compare our algorithm with the two recent semi-supervised approaches proposed in [5,13], which are both based on pseudo-labeling. Namely, a fully-supervised trained model produces pseudo-labels for the unlabeled data, and then the model is

retrained on the labeled and pseudo-labeled data. The difference between both methods is that [13], denoted by ABINet_{est} , filters out pseudo-labels of low confidence level, while [5], denoted as ABINet_{PL} , uses all the pseudo-labels. For a fair comparison, we reimplement both training schemes and apply them to the same text recognition architecture and training sets. Additional implementation details are listed in Appendix C.

As shown in Table 2, leveraging the unlabeled real-world data significantly boosts performance, although these images mainly come (88%) from book covers, a different domain to the test sets. The comparison between the semi-supervised methods (Real-L + Real-U) shows that our method consistently improves performance across all the common and non-common benchmarks. This performance gain is achieved even though SemiMTR requires fewer training stages, as it does not involve a retraining stage.

We further analyze our method and examine the performance gain of leveraging unlabeled data only at the vision model pretraining, which we named *SemiMTR-V*, and only at the fine-tuning stage, denoted as *SemiMTR-F*. As presented in Table 2, each of these parts efficiently utilizes unlabeled data. In fact, each of these partial versions of our algorithm reaches a higher overall average accuracy, calculated across common and non-common benchmarks, than the current semi-supervised algorithms. Nevertheless, as mentioned above, our complete algorithm surpasses these results and presents improved performance on 12 out of 13 benchmarks. This analysis confirms our claim that full utilization of unlabeled data requires a semi-supervised training scheme that pays attention to the multimodal structure.

At this point, the reader might wonder about the applicability of the current synthetic datasets. To answer this question, we examine an additional training configuration, in which we utilize all labeled real-world and synthetic data along with the unlabeled real-world data (Real-L + Synth + Real-U). Harnessing also the synthetic data leads to average accuracy improvements of +0.9% on common benchmarks and of +0.4% on non-common. These results indicate that the labeled real-world datasets of scene text recognition are still in the low data regime and, therefore, can be contributed by synthetic alternatives.

6 Ablation Studies

In this section, we examine the impact of the main components of SemiMTR. All the experiments here use labeled and unlabeled real-world data (Real-L + Real-U). While, for brevity, we report only the weighted average accuracies on the common and non-common benchmarks.

6.1 Vision Model Pretraining

Two-stage versus unified training. Standard contrastive learning methods [9,16,14,8], including SeqCLR [1], are based on the two training stages of contrastive-based pretraining and fully-supervised fine-tuning. In contrast to this

Table 3: **Ablation of vision model pretraining.** Accuracy of the vision model when pretrained via a typical two-stage scheme versus our unified method and when using different augmentation pipelines

Method	Augmentations	Vision Model	
		Common Benchmarks	Non-Common Benchmarks
<i>Supervised Baseline</i> [13]	ABINet [13]	85.3	57.9
Two-Stage	SeqCLR [1]	86.7	59.6
Unified	SeqCLR [1]	87.0	60.2
Unified	Ours	88.1	60.3

Table 4: **Consistency loss ablation.** Accuracy of different consistency loss configurations, calculated on both the common and non-common benchmarks

Consistency Loss	Stop Gradients	Soft labels	Threshold	Common Benchmarks	Non-Common Benchmarks
CE	✓	✗	✗	91.8	65.0
CE	✗	✓	✗	91.8	64.1
CE	✓	✓	✗	91.8	64.5
KL Divergence	✗	✓	✗	92.2	64.5
CE	✓	✗	✓	92.2	65.0
CE	✗	✓	✓	92.0	65.0
CE	✓	✓	✓	92.0	64.7
KL Divergence	✗	✓	✓	92.1	64.8

scheme, we propose a unified training stage for the vision model pretraining, combining the contrastive learning objective with the supervised cross-entropy loss, as defined in Eq. (4). By doing so, we maintain that the overall training algorithm consists of three stages, similar to the origin ABINet training [13]. We present in Table 3 the experimental comparison between these training approaches. As shown, the unified training stage even leads to performance improvements.

Augmentation. While handwritten text images, which SeqCLR [1] mainly focuses on, are usually of light-color solid background, text-in-the-wild images are often colorful with unique backgrounds. This substantial domain difference leads us to suggest stronger color-texture augmentations, which are needed for learning effective representations that focus on the text content and not the general visual attributes. Table 3 shows the performance gain of the proposed augmentation technique compared to the origin SeqCLR augmentation pipeline [1].

6.2 Consistency Regularization

Sequential consistency regularization loss. Here, we examine the contributions of the different ingredients of the proposed sequential consistency loss, defined in Eq. (5). In particular, we compare cross-entropy with KL-divergence

Table 5: **Teacher-student identities.** Accuracy attained by varying teacher and student identities

Teacher	Student	Common Benchmarks	Non-Common Benchmarks
Vision	Vision	91.7	64.8
Vision	Language	91.9	64.5
Vision	Fusion	92.1	65.2
Vision	Vision, Language, Fusion	91.8	65.0
Fusion	Vision	92.0	64.7
Fusion	Language	91.7	64.6
Fusion	Fusion	92.2	65.1
Fusion	Vision, Language, Fusion	92.3	65.1
Vision, Language, Fusion	Vision, Language, Fusion	92.4	65.2

and soft labels (probabilities vectors) versus one-hot labels. In addition, we investigate stopping the teacher gradients and using a threshold. In these experiments, the vision model is the teacher modality that generates the pseudo-labels, and all the modalities are the students trained on these pseudo-labels. As shown in Table 4, in our setting, KL divergence as the core loss function instead of cross-entropy does not lead to consistent improvements. Moreover, adding a certainty-based threshold for the teacher predictions (set to 90%) stabilizes results; however, it has a marginal effect in the best configuration that consists of cross-entropy, stop gradients, and uses one-hot (hard) labels.

Teacher-student modalities. In unimodal architectures, the teacher and student identity are usually clear since such models contain a single output. Nevertheless, in multimodal architectures, each modality output can be the teacher or the student. In Table 5, we examine several of the possible teacher-student configurations and reveal that the most effective learning occurs when each modality is a teacher of its own. Meaning, that each modality generates its own pseudo-labels to train on, as defined in Eq. (6).

7 Conclusions and Future Work

We present SemiMTR, the first multimodal tailored, semi-supervised learning algorithm for text recognition. To this end, we introduce a novel contrastive-based visual representation learning for scene text and a sequential, character-level consistency regularization. Although it leverages unlabeled data in addition to labeled one, our method maintains a compact three-stage algorithm. Comprehensive experiments demonstrate that SemiMTR outperforms supervised and semi-supervised state-of-the-art methods on multiple scene text recognition benchmarks. We believe that the success of SemiMTR will encourage researchers to further explore schemes for leveraging labeled and unlabeled real-world data for scene text recognition. In addition, our work sheds light on the status of current synthetic and real-world datasets, which can help future dataset creators.

References

1. Aberdam, A., Litman, R., Tsiper, S., Anshel, O., Slossberg, R., Mazor, S., Manmatha, R., Perona, P.: Sequence-to-sequence contrastive learning for text recognition. In: Proceedings of the IEEE/CVF Conference on Computer Vision and Pattern Recognition. pp. 15302–15312 (2021) [2](#), [3](#), [5](#), [6](#), [7](#), [8](#), [12](#), [13](#), [23](#)
2. Atienza, R.: Vision transformer for fast and efficient scene text recognition. In: International Conference on Document Analysis and Recognition. pp. 319–334. Springer (2021) [6](#)
3. Bachman, P., Alsharif, O., Precup, D.: Learning with pseudo-ensembles (2014) [4](#)
4. Baek, J., Kim, G., Lee, J., Park, S., Han, D., Yun, S., Oh, S.J., Lee, H.: What is wrong with scene text recognition model comparisons? dataset and model analysis. In: Proceedings of the IEEE International Conference on Computer Vision. pp. 4715–4723 (2019) [2](#), [3](#), [11](#)
5. Baek, J., Matsui, Y., Aizawa, K.: What if we only use real datasets for scene text recognition? toward scene text recognition with fewer labels. In: Proceedings of the IEEE/CVF Conference on Computer Vision and Pattern Recognition. pp. 3113–3122 (2021) [2](#), [3](#), [5](#), [9](#), [10](#), [11](#), [12](#), [21](#)
6. Berthelot, D., Carlini, N., Goodfellow, I., Papernot, N., Oliver, A., Raffel, C.: Mixmatch: A holistic approach to semi-supervised learning (2019) [4](#)
7. Biten, A.F., Tito, R., Mafla, A., Gomez, L., Rusinol, M., Valveny, E., Jawahar, C., Karatzas, D.: Scene text visual question answering. In: Proceedings of the IEEE/CVF international conference on computer vision. pp. 4291–4301 (2019) [10](#)
8. Caron, M., Misra, I., Mairal, J., Goyal, P., Bojanowski, P., Joulin, A.: Unsupervised learning of visual features by contrasting cluster assignments. *Advances in Neural Information Processing Systems* **33**, 9912–9924 (2020) [7](#), [8](#), [12](#)
9. Chen, T., Kornblith, S., Norouzi, M., Hinton, G.: A simple framework for contrastive learning of visual representations. In: International conference on machine learning. pp. 1597–1607. PMLR (2020) [2](#), [7](#), [8](#), [12](#)
10. Chen, X., Jin, L., Zhu, Y., Luo, C., Wang, T.: Text recognition in the wild: A survey. arXiv preprint arXiv:2005.03492 (2020) [1](#)
11. Chng, C.K., Liu, Y., Sun, Y., Ng, C.C., Luo, C., Ni, Z., Fang, C., Zhang, S., Han, J., Ding, E., et al.: Icdar2019 robust reading challenge on arbitrary-shaped text-rrc-art. In: 2019 International Conference on Document Analysis and Recognition (ICDAR). pp. 1571–1576. IEEE (2019) [10](#)
12. Devlin, J., Chang, M.W., Lee, K., Toutanova, K.: Bert: Pre-training of deep bidirectional transformers for language understanding. arXiv preprint arXiv:1810.04805 (2018) [4](#)
13. Fang, S., Xie, H., Wang, Y., Mao, Z., Zhang, Y.: Read like humans: autonomous, bidirectional and iterative language modeling for scene text recognition. In: Proceedings of the IEEE/CVF Conference on Computer Vision and Pattern Recognition. pp. 7098–7107 (2021) [2](#), [3](#), [4](#), [5](#), [6](#), [9](#), [10](#), [11](#), [12](#), [13](#), [19](#), [20](#), [21](#), [22](#), [23](#)
14. Grill, J.B., Strub, F., Altché, F., Tallec, C., Richemond, P., Buchatskaya, E., Doersch, C., Avila Pires, B., Guo, Z., Gheshlaghi Azar, M., et al.: Bootstrap your own latent—a new approach to self-supervised learning. *Advances in Neural Information Processing Systems* **33**, 21271–21284 (2020) [7](#), [8](#), [12](#)
15. Gupta, A., Vedaldi, A., Zisserman, A.: Synthetic data for text localisation in natural images. In: Proceedings of the IEEE conference on computer vision and pattern recognition. pp. 2315–2324 (2016) [3](#), [10](#)

16. He, K., Fan, H., Wu, Y., Xie, S., Girshick, R.: Momentum contrast for unsupervised visual representation learning. In: Proceedings of the IEEE/CVF conference on computer vision and pattern recognition. pp. 9729–9738 (2020) [2](#), [7](#), [8](#), [12](#)
17. Iwana, B.K., Rizvi, S.T.R., Ahmed, S., Dengel, A., Uchida, S.: Judging a book by its cover. arXiv preprint arXiv:1610.09204 (2016) [10](#)
18. Jaderberg, M., Simonyan, K., Vedaldi, A., Zisserman, A.: Synthetic data and artificial neural networks for natural scene text recognition. arXiv preprint arXiv:1406.2227 (2014) [3](#), [10](#)
19. Janouskova, K., Matas, J., Gomez, L., Karatzas, D.: Text recognition-real world data and where to find them. In: 2020 25th International Conference on Pattern Recognition (ICPR). pp. 4489–4496. IEEE (2021) [3](#)
20. Jung, A.B., Wada, K., Crall, J., Tanaka, S., Graving, J., Reinders, C., Yadav, S., Banerjee, J., Vecsei, G., Kraft, A., Rui, Z., Borovec, J., Vallentin, C., Zhydenko, S., Pfeiffer, K., Cook, B., Fernández, I., De Rainville, F.M., Weng, C.H., Ayala-Acevedo, A., Meudec, R., Laporte, M., et al.: [ingaug](https://github.com/aleju/ingaug) (2020), online; accessed 01-Feb-2020 [21](#)
21. Kang, L., Rusiñol, M., Fornés, A., Riba, P., Villegas, M.: Unsupervised adaptation for synthetic-to-real handwritten word recognition. In: 2020 IEEE Winter Conference on Applications of Computer Vision (WACV). pp. 3491–3500. IEEE (2020) [3](#)
22. Karatzas, D., Gomez-Bigorda, L., Nicolaou, A., Ghosh, S., Bagdanov, A., Iwamura, M., Matas, J., Neumann, L., Chandrasekhar, V.R., Lu, S., et al.: Icdar 2015 competition on robust reading. In: 2015 13th International Conference on Document Analysis and Recognition (ICDAR). pp. 1156–1160. IEEE (2015) [10](#)
23. Karatzas, D., Shafait, F., Uchida, S., Iwamura, M., i Bigorda, L.G., Mestre, S.R., Mas, J., Mota, D.F., Almazan, J.A., De Las Heras, L.P.: Icdar 2013 robust reading competition. In: 2013 12th International Conference on Document Analysis and Recognition. pp. 1484–1493. IEEE (2013) [10](#)
24. Laine, S., Aila, T.: Temporal ensembling for semi-supervised learning. arXiv preprint arXiv:1610.02242 (2016) [4](#)
25. Lee, J., Park, S., Baek, J., Oh, S.J., Kim, S., Lee, H.: On recognizing texts of arbitrary shapes with 2d self-attention. In: Proceedings of the IEEE/CVF Conference on Computer Vision and Pattern Recognition Workshops. pp. 546–547 (2020) [6](#)
26. Li, H., Wang, P., Shen, C., Zhang, G.: Show, attend and read: A simple and strong baseline for irregular text recognition. In: AAAI (2019) [2](#), [3](#)
27. Liao, M., Lyu, P., He, M., Yao, C., Wu, W., Bai, X.: Mask textspotter: An end-to-end trainable neural network for spotting text with arbitrary shapes. TPAMI (2019) [2](#), [3](#)
28. Litman, R., Anschel, O., Tsiper, S., Litman, R., Mazor, S., Manmatha, R.: Scatter: selective context attentional scene text recognizer. In: proceedings of the IEEE/CVF conference on computer vision and pattern recognition. pp. 11962–11972 (2020) [2](#), [3](#), [11](#)
29. Long, S., He, X., Ya, C.: Scene text detection and recognition: The deep learning era. arXiv preprint arXiv:1811.04256 (2018) [1](#)
30. Lucas, S.M., Panaretos, A., Sosa, L., Tang, A., Wong, S., Young, R.: Icdar 2003 robust reading competitions. In: Seventh International Conference on Document Analysis and Recognition, 2003. Proceedings. pp. 682–687. Citeseer (2003) [10](#)
31. Lyu, P., Yang, Z., Leng, X., Wu, X., Li, R., Shen, X.: 2d attentional irregular scene text recognizer. arXiv preprint arXiv:1906.05708 (2019) [19](#)
32. Merity, S., Xiong, C., Bradbury, J., Socher, R.: Pointer sentinel mixture models (2016) [20](#)

33. Mishra, A., Alahari, K., Jawahar, C.: Scene text recognition using higher order language priors (2012) [10](#)
34. Mou, Y., Tan, L., Yang, H., Chen, J., Liu, L., Yan, R., Huang, Y.: Plugnet: Degradation aware scene text recognition supervised by a pluggable super-resolution unit. In: European Conference on Computer Vision. pp. 158–174. Springer (2020) [2](#), [11](#)
35. Nayef, N., Patel, Y., Busta, M., Chowdhury, P.N., Karatzas, D., Khlif, W., Matas, J., Pal, U., Burie, J.C., Liu, C.I., et al.: Icdar2019 robust reading challenge on multilingual scene text detection and recognition—rrc-mlt-2019. In: 2019 International conference on document analysis and recognition (ICDAR). pp. 1582–1587. IEEE (2019) [10](#)
36. Nuriel, O., Fogel, S., Litman, R.: Textadain: Fine-grained adain for robust text recognition. arXiv preprint arXiv:2105.03906 (2021) [3](#)
37. Oord, A.v.d., Li, Y., Vinyals, O.: Representation learning with contrastive predictive coding. arXiv preprint arXiv:1807.03748 (2018) [7](#)
38. Qiao, Z., Zhou, Y., Yang, D., Zhou, Y., Wang, W.: Seed: Semantics enhanced encoder-decoder framework for scene text recognition. In: Proceedings of the IEEE/CVF Conference on Computer Vision and Pattern Recognition. pp. 13528–13537 (2020) [2](#), [3](#)
39. Quy Phan, T., Shivakumara, P., Tian, S., Lim Tan, C.: Recognizing text with perspective distortion in natural scenes. In: Proceedings of the IEEE International Conference on Computer Vision. pp. 569–576 (2013) [10](#)
40. Risnumawan, A., Shivakumara, P., Chan, C.S., Tan, C.L.: A robust arbitrary text detection system for natural scene images. Expert Systems with Applications **41**(18), 8027–8048 (2014) [10](#)
41. Ronneberger, O., Fischer, P., Brox, T.: U-net: Convolutional networks for biomedical image segmentation. In: International Conference on Medical image computing and computer-assisted intervention. pp. 234–241. Springer (2015) [19](#)
42. Sajjadi, M., Javanmardi, M., Tasdizen, T.: Regularization with stochastic transformations and perturbations for deep semi-supervised learning. Advances in neural information processing systems **29** (2016) [4](#)
43. Sengupta, P., Mollah, A.F.: Journey of scene text components recognition: Progress and open issues. Multimedia Tools and Applications pp. 1–26 (2020) [1](#)
44. Shi, B., Bai, X., Yao, C.: An end-to-end trainable neural network for image-based sequence recognition and its application to scene text recognition. IEEE transactions on pattern analysis and machine intelligence **39**(11), 2298–2304 (2016) [2](#), [3](#)
45. Shi, B., Yang, M., Wang, X., Lyu, P., Yao, C., Bai, X.: Aster: An attentional scene text recognizer with flexible rectification. TPAMI (2018) [2](#), [3](#), [19](#)
46. Shi, B., Yao, C., Liao, M., Yang, M., Xu, P., Cui, L., Belongie, S., Lu, S., Bai, X.: Icdar2017 competition on reading chinese text in the wild (rctw-17). In: 2017 14th iapr international conference on document analysis and recognition (ICDAR). vol. 1, pp. 1429–1434. IEEE (2017) [10](#)
47. Singh, A., Natarajan, V., Shah, M., Jiang, Y., Chen, X., Batra, D., Parikh, D., Rohrbach, M.: Towards vqa models that can read. In: Proceedings of the IEEE/CVF Conference on Computer Vision and Pattern Recognition. pp. 8317–8326 (2019) [10](#)
48. Sohn, K., Berthelot, D., Carlini, N., Zhang, Z., Zhang, H., Raffel, C.A., Cubuk, E.D., Kurakin, A., Li, C.L.: Fixmatch: Simplifying semi-supervised learning with consistency and confidence. Advances in Neural Information Processing Systems **33**, 596–608 (2020) [4](#)

49. Sun, Y., Ni, Z., Chng, C.K., Liu, Y., Luo, C., Ng, C.C., Han, J., Ding, E., Liu, J., Karatzas, D., et al.: Icdar 2019 competition on large-scale street view text with partial labeling-rrc-lsvt. In: 2019 International Conference on Document Analysis and Recognition (ICDAR). pp. 1557–1562. IEEE (2019) [10](#)
50. Tarvainen, A., Valpola, H.: Mean teachers are better role models: Weight-averaged consistency targets improve semi-supervised deep learning results. *Advances in neural information processing systems* **30** (2017) [4](#)
51. Vaswani, A., Shazeer, N., Parmar, N., Uszkoreit, J., Jones, L., Gomez, A.N., Kaiser, L., Polosukhin, I.: Attention is all you need. *Advances in neural information processing systems* **30** (2017) [19](#)
52. Veit, A., Matera, T., Neumann, L., Matas, J., Belongie, S.: Coco-text: Dataset and benchmark for text detection and recognition in natural images. *arXiv preprint arXiv:1601.07140* (2016) [10](#)
53. Wan, Z., He, M., Chen, H., Bai, X., Yao, C.: Textscanner: Reading characters in order for robust scene text recognition. In: *AAAI* (2020) [2, 3](#)
54. Wang, K., Babenko, B., Belongie, S.: End-to-end scene text recognition. In: 2011 International Conference on Computer Vision. pp. 1457–1464. IEEE (2011) [10](#)
55. Wang, T., Zhu, Y., Jin, L., Luo, C., Chen, X., Wu, Y., Wang, Q., Cai, M.: Decoupled attention network for text recognition. In: *AAAI* (2020) [2, 3](#)
56. Wang, Y., Xie, H., Fang, S., Wang, J., Zhu, S., Zhang, Y.: From two to one: A new scene text recognizer with visual language modeling network. In: *Proceedings of the IEEE/CVF International Conference on Computer Vision*. pp. 14194–14203 (2021) [2, 3, 11](#)
57. Xie, Q., Dai, Z., Hovy, E., Luong, T., Le, Q.: Unsupervised data augmentation for consistency training. *Advances in Neural Information Processing Systems* **33**, 6256–6268 (2020) [4](#)
58. Yang, M., Guan, Y., Liao, M., He, X., Bian, K., Bai, S., Yao, C., Bai, X.: Symmetry-constrained rectification network for scene text recognition. In: *ICCV* (2019) [2, 3](#)
59. Yu, D., Li, X., Zhang, C., Liu, T., Han, J., Liu, J., Ding, E.: Towards accurate scene text recognition with semantic reasoning networks. In: *Proceedings of the IEEE/CVF Conference on Computer Vision and Pattern Recognition*. pp. 12113–12122 (2020) [2, 3, 11, 19](#)
60. Yue, X., Kuang, Z., Lin, C., Sun, H., Zhang, W.: Robustscanner: Dynamically enhancing positional clues for robust text recognition. In: *ECCV* (2020) [2, 3](#)
61. Yue, X., Kuang, Z., Lin, C., Sun, H., Zhang, W.: Robustscanner: Dynamically enhancing positional clues for robust text recognition. In: *European Conference on Computer Vision*. pp. 135–151. Springer (2020) [11](#)
62. Zhan, F., Lu, S.: Esir: End-to-end scene text recognition via iterative image rectification. In: *CVPR* (2019) [2, 3](#)
63. Zhang, R., Zhou, Y., Jiang, Q., Song, Q., Li, N., Zhou, K., Wang, L., Wang, D., Liao, M., Yang, M., et al.: Icdar 2019 robust reading challenge on reading chinese text on signboard. In: 2019 international conference on document analysis and recognition (ICDAR). pp. 1577–1581. IEEE (2019) [10](#)
64. Zhang, Y., Nie, S., Liu, W., Xu, X., Zhang, D., Shen, H.T.: Sequence-to-sequence domain adaptation network for robust text image recognition. In: *Proceedings of the IEEE Conference on Computer Vision and Pattern Recognition*. pp. 2740–2749 (2019) [2, 3](#)
65. Zhang, Y., Gueguen, L., Zharkov, I., Zhang, P., Seifert, K., Kadlec, B.: Uber-text: A large-scale dataset for optical character recognition from street-level imagery. In: *SUNw: Scene Understanding Workshop-CVPR*. vol. 2017, p. 5 (2017) [10](#)

A ABINet Architecture

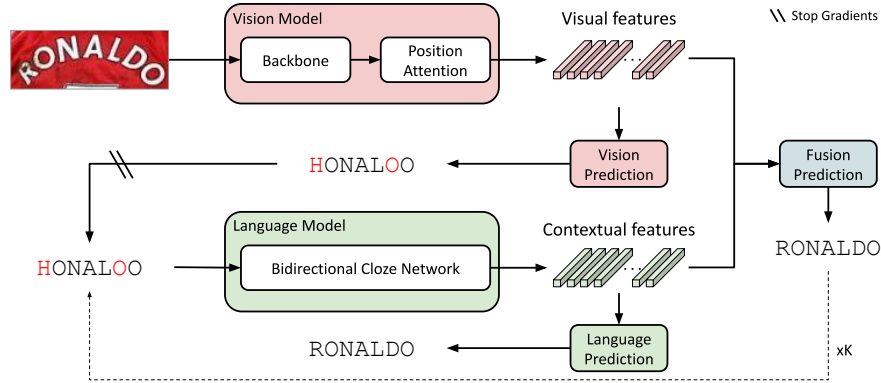


Fig. 5: **ABINet text recognition architecture.** As mentioned in the main paper and repeated here for convenient, we adopt ABINet [13] as our case study of vision-language multimodal recognizers. In this scheme, the vision model first extracts a sequence of visual features from a given image and then decodes it into character predictions. Next, these predictions are fed to the language model, which derives contextual features. Finally, the fusion model operates on the visual and contextual features and provides the network final prediction. To further improve accuracy, an optional iterative phase, drawn with a dashed line, reinserts the output back to the language model as a predictions-refinement step

In our work we adopt the ABINet-LV, which depicted here again, Fig. 5, for convenient. This architecture consists of the following three models:

1. **Vision Model** consists of backbone network and position attention. The visual backbone comprises ResNet [45] and Transformer units [31,59]. Thus, the visual backbone features for a given image $\mathbf{X} \in \mathbb{R}^{3 \times H \times W}$ are:

$$\mathbf{F}_b = \text{Transformer}(\text{ResNet}(\mathbf{X})) \in \mathbb{R}^{\frac{H}{4} \times \frac{W}{4} \times C}, \quad (7)$$

where C is the feature dimension. Then, the position attention module, which is based on the query paradigm [51], is applied on \mathbf{F}_b to produce the visual features:

$$\mathbf{F}_v = \text{softmax} \left(\frac{\mathbf{Q}\mathbf{K}^T}{\sqrt{C}} \right) \text{Flatten}(\mathbf{F}_b) \in \mathbb{R}^{T \times C}, \quad (8)$$

where $\mathbf{K} = \text{Mini U-Net}(\mathbf{F}_b) \in \mathbb{R}^{\frac{HW}{16} \times C}$ [41], T is the character sequence length, and $\mathbf{Q} \in \mathbb{R}^{T \times C}$ is the positional encoding of the character orders. Finally, a sequence of linear classifier and softmax operator transcribes the visual features into character probabilities in parallel. These character probabilities are fed to the language model as a seed text generator.

2. **Language Model** is a variant of L -layers transformer decoder ($L = 4$ in our case), named bidirectional cloze network (BCN). The input to this model is the visual predictions in the first iteration, while in next iterations is the fusion model predictions. As before, a linear layer and softmax operates on the contextual features, $\mathbf{F}_l \in \mathbb{R}^{T \times C}$ to provide character probabilities. We refer the reader to Appendix B for additional details.
3. **Fusion Model**, a gated mechanism which operates on the visual and contextual features and produces the align features. As depicted in Fig. 5, the fusion predictions can be inserted again to the language model in an iterative correction manner. Therefore, this model can be written as,

$$\mathbf{G} = \sigma([\mathbf{F}_v, \mathbf{F}_l^i] \mathbf{W}_f) \quad (9)$$

$$\mathbf{F}_f^i = \mathbf{G} \odot \mathbf{F}_v + (1 - \mathbf{G}) \odot \mathbf{F}_l^i, \quad (10)$$

where \odot denotes the Hadamard (element-wise) product and i is the iteration number out of K total ($K = 3$ in our case).

We refer the reader to ABINet work [13] for more details.

B Language Model Pretraining

One of the main themes advocated in ABINet [13] is that the language model (LM) should be decoupled from the vision one and trained explicitly to learn linguistic rules. Such modality-separation enables to harness the remarkable improvements attained in training LM in Natural Language Processing and to pretrain it on a large text corpus. More specifically, the LM pretraining is based on bidirectional representation learning using a masked language model (MLM). A possible, straightforward way to do so is by masking a certain input text token and training the LM to predict it. Nevertheless, doing so requires applying such masking n for a sentence of length n . To mitigate this overhead, ABINet proposes to apply the masking on the attention maps of the LM architecture – when predicting output i , the attention mask prevents the model from receiving information from input i , and thus, implements the MLM efficiently.

The LM is trained using MLM on a filtered version of WikiText-103 [32] corpus (applying basic filtering – word’s size and unsupported characters), that contains 86.5 million text tokens. The model is pretrained for 80 epochs, using a batch size of 4096, Adam optimizer ($\beta_1 = 0.9, \beta_2 = 0.999$), no weight decay, gradient clipping of 20, and initial learning rate of 0.0001 with a drop (multiplying it by 0.1) at epoch 70.

C Comparison to State-of-the-art Semi-Supervised

Scene Text: In this section, we provide additional implementation and technical details, regarding the reproduction of the semi-supervised methods, denoted

as ABINet_{PL} [5] and ABINet_{est} [13]. In both of these, we fine-tune ABINet using a pretrained language model and a pretrained visual model, trained on the labeled portion (X^l, Y^l) . Then, we use it to predict the unlabeled portion X^u and construct a unified dataset, wherein ABINet_{est} , we apply certainty-based filtering, as proposed in [13]. More specifically, we filter out pseudo labels with a text certainty \mathcal{C} below predefined value Q (we set $Q = 0.9$, as in the original paper). The text certainty of a pseudo label is defined as the minimal certainty of its characters, denoted as $c(t)$. The characters' certainty is the maximal over the prediction of all the iterations of ABINet (the certainty of the i -th character of the k -th iteration is denoted as $c(t, k)$). This filtering mechanism description is depicted in Equation 11 below.

$$\begin{aligned} c(t) &= \max_{1 \leq k \leq K} c(t, k) \\ \mathcal{C} &= \min_{1 \leq t \leq T} c(t) \end{aligned} \tag{11}$$

Where K is the number of ABINet's iterations and T is the effective length of the pseudo label. Finally, we use the pretrained vision and language models and fine-tune the ABINet using the unified dataset. These semi-supervised methods are described in Algorithms 1 and 2.

Algorithm 1 ABINet_{PL}

Inputs: Labeled data (X^l, Y^l) and unlabeled data X^u .

- 1: Pretrain vision model on (X^l, Y^l)
 - 2: Fine-tune ABINet on (X^l, Y^l)
 - 3: Use ABINet to generate pseudo-labels (Y^u) on X^u
 - 4: $(X, Y) \leftarrow \{(X^l, Y^l) \cup (X^u, Y^u)\}$
 - 5: Retrain ABINet on (X, Y)
-

Algorithm 2 ABINet_{est}

Inputs: Labeled data (X^l, Y^l) and unlabeled data X^u .

- 1: Pretrain vision model on (X^l, Y^l)
 - 2: Fine-tune ABINet on (X^l, Y^l)
 - 3: Use ABINet to generate pseudo-labels (Y^u) on X^u
 - 4: Filter (X^u, Y^u) using Eq. (11)
 - 5: $(X, Y) \leftarrow \{(X^l, Y^l) \cup (X^u, Y^u)\}$
 - 6: Retrain ABINet on (X, Y)
-

D Data

As mentioned in the main paper, in this work we consider the same datasets used by Beak et al. [5]. In particular, we use the Synth, Real-L and Real-U datasets, see examples from each in Fig. 6.

E Augmentations

A pseudo-code for the augmentation pipeline, written with the `imgaug` [20] package, is as follows.

```

1 from imgaug import augmenters as iaa
2

```

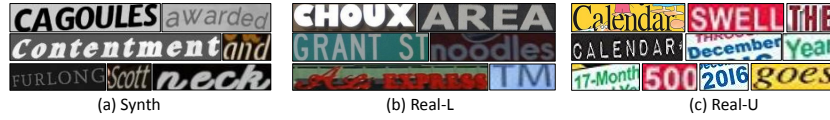


Fig. 6: **Dataset samples.** We provide examples from each of the datasets used in this work, namely; (a) Synth, (b) Real-L and (c) Real-U

```

3
4 iaa.Sequential([
5     iaa.Invert(0.5),
6     iaa.OneOf([
7         iaa.ChannelShuffle(0.35),
8         iaa.Grayscale(alpha=(0.0, 1.0)),
9         iaa.KMeansColorQuantization(),
10        iaa.HistogramEqualization(),
11        iaa.Dropout(p=(0, 0.2), per_channel=0.5),
12        iaa.GammaContrast((0.5, 2.0)),
13        iaa.MultiplyBrightness((0.5, 1.5)),
14        iaa.AddToHueAndSaturation((-50, 50), per_channel=True)
15    ]),
16     iaa.ChangeColorTemperature((1100, 10000))
17 ]),
18 iaa.OneOf([
19     iaa.Sharpen(alpha=(0.0, 0.5), lightness=(0.0, 0.5)),
20     iaa.OneOf([
21         iaa.GaussianBlur((0.5, 1.5)),
22         iaa.AverageBlur(k=(2, 6)),
23         iaa.MedianBlur(k=(3, 7)),
24         iaa.MotionBlur(k=5)
25     ])
26 ]),
27 iaa.OneOf([
28     iaa.Emboss(alpha=(0.0, 1.0), strength=(0.5, 1.5)),
29     iaa.AdditiveGaussianNoise(scale=(0, 0.2 * 255)),
30     iaa.ImpulseNoise(0.1),
31     iaa.MultiplyElementwise((0.5, 1.5))
32 ])

```

F Implementation Details

As baseline, we use the code of ABINet³ [13], and our architectural changes are implemented on top of ABINet-LV. All experiments are trained and tested using the PyTorch⁴ framework on 4 Tesla V100 GPUs with 16GB memory each.

³ <https://github.com/FangShancheng/ABINet>

⁴ <https://pytorch.org/>

The model dimension C is set to 512 throughout. There are 4 layers in BCN with 8 attention heads each layer. Images are directly resized to 32×128 . We train using the ADAM optimizer with the initial learning rate of $1e^{-4}$, decay rate of 0.1, and gradient clipping of a magnitude of 20. The number of character classes is 37; 10 for digits, 26 for alphabets, and a single padding token. All the coefficient scalars are set to 1.

For the vision pretraining, the batch size is 304 with a sampling ratio of 30%, 70% between the labeled and unlabeled data, respectively. The number of epochs is 25 with scheduler periods of [17, 5, 3]. The SeqCLR head [1] does not contain a projection head, the temperature parameter is $\tau = 0.1$, and the window-to-instance mapping function outputs $T = 5$ instances for each feature map.

We use the pretrained language model provide by [13]. For the fusion training, the batch size is 232 with a sampling ratio of 30%, 70% between the labeled and unlabeled data, respectively. The number of epochs is 5 with scheduler periods of [3, 1, 1]. As for augmentation, we refer the reader to Appendix E for more details.